Multiple Ligand and Cell-Dependent States of Lateral Mobility of Plasmalemmal G Protein-Coupled Cholecystokinin Receptors

Belinda F. Roettger,[1] Edward H. Hellen,[1] Thomas P. Burghardt,[1] and Laurence J. Miller[1,2]

Lateral movement of receptor molecules in the plane of the plasmalemma has important implications for signal transduction and receptor regulation, yet mechanisms affecting such movement are not well understood. We have studied the lateral mobility of the G protein-coupled cholecystokinin (CCK) receptor expressed in the natural milieu of the rat pancreatic acinar cell and in a model cell system, the CHO-CCKR cell, after occupation with fluorescent agonist and antagonist. Lateral diffusion characteristics were distinct in each type of cell and for receptors occupied by each type of ligand, fluorescent agonist, rhodamine-Gly-[(Nle^{28,31})CCK-26-33], and fluorescent antagonist, rhodamine-Gly-[(D-Trp^{30},Nle^{28,31})CCK-26-32]-phenethyl ester. Multiple states of mobility were detected for CCK receptors. The slowest population of mobile receptors on the CHO-CCKR cells moved at similar rates when occupied by both antagonist and agonist, while the faster-moving populations moved at a faster rate when occupied with antagonist than with agonist. The fastest component of mobile receptors may reflect unconstrained interactions of the antagonist-occupied receptors with signaling or anchoring structures, while the slowest component may represent the fraction of ligand-occupied receptors that ultimately undergo internalization. The intermediate mobility states may reflect receptor interactions with signal transduction and regulatory machinery. While only a single population of mobile receptors was demonstrable on the acinar cells, increased ligand concentrations (agonist and antagonist) resulted in increased percentages of mobile receptors, suggesting a stoichiometric limitation of immobilizing molecular constraints. Inhibition of protein kinase C had no significant effect on the lateral mobility of agonist-occupied CCK receptors.

KEY WORDS: Fluorescence recovery after photobleaching; G protein-coupled receptors; lateral mobility; membrane receptors.

INTRODUCTION

Peptide hormone receptors reside in the plasma membrane, where their lateral mobility has been impli-cated in key signaling and regulatory events. While still within the plasma membrane, receptors may undergo dimerization or association with proximal effector or other regulatory molecules. The list of molecules shown to interact with guanine nucleotide-binding protein (G protein)-coupled receptors and components of its well-recognized ternary complex has expanded dramatically in recent years [1–9]. Membrane events may also contrib-ute to receptor desensitization by uncoupling the receptor from proximal effectors, insulating the receptor in a unique plasmalemmal microdomain, or initiating receptor

[1] Center for Basic Research in Digestive Diseases and Department of Biochemistry and Molecular Biology, Mayo Clinic and Foundation, Rochester, Minnesota 55905.
[2] To whom correspondence should be addressed at Center for Basic Research in Digestive Diseases, Guggenheim 17, Mayo Clinic, Roch-ester, Minnesota 55905. Fax: (507)-284-0762. E-mail: miller@mayo.edu

movement off the cell surface via endocytosis [10–12]. The cellular and molecular determinants for these processes are not well understood.

We have considerable information about the movement of the G protein-coupled cholecystokinin (CCK) receptor following occupation with a full agonist [11]. This receptor stimulates phospholipase C, protein kinase C, and a rise in intracellular calcium and is physiologically important in mediating pancreatic exocrine secretion, gallbladder contraction, enteric motility, and satiety [13]. We have demonstrated that the CCK receptor is highly mobile in the plane of the plasma membrane, moving laterally with an apparent diffusion coefficient of the order of $1 \times 10^{-10} \, cm^2/s$ [11]. Following activation, most agonist-occupied receptors are internalized via clathrin-dependent endocytosis, while a minor population moves into caveolae in recombinant CCK receptor-bearing Chinese hamster ovary (CHO-CCKR) cells [12]. In the natural environment of the pancreatic acinar cell, CCK receptors are laterally mobile with a diffusion coefficient similar to that measured in CHO-CCKR cells, however, rather than undergoing endocytosis, these receptors become immobilized in a novel microdomain of the plasma membrane, via a process termed "insulation" [11].

In this work, we have explored the mobility of this receptor on these same cells when occupied by an antagonist ligand and have extended our previous observations and analysis of lateral mobility of the CCK receptor occupied by a full agonist. This includes a careful analysis of the possibility of multiple states of lateral mobility of the receptor and of variables that might affect apparent mobility measured by observations of fluorescent ligands. The fluorescent antagonist used in this work, rhodamine-Gly-[(D-Trp^{30},Nle^{28,31})CCK-26-32]-phenethyl ester (Rho-D-Trp-OPE), is an analogue of JMV-179 [14] that we have characterized previously [15]. The mobility of the CCK receptor occupied by this reagent was compared to that of the same receptor occupied with the fluorescent full agonist, rhodamine-Gly-[(Nle^{28,31})CCK-26-33] (Rho-CCK). A series of experiments was also performed to explore the role of protein kinase C in receptor mobility.

EXPERIMENTAL

Reagents. Bovine serum albumin Cohn fraction V was purchased from Intergen Co. (Purchase, NY), soybean trypsin inhibitor and collagenase were from Worthington Biochemical Corp. (Freehold, NJ), and 5,6-carboxytetramethyl rhodamine succinimide was from Molecular Probes, Inc. (Eugene, OR). Tissue culture supplies were from GIBCO-BRL (Gaithersburg, MD), except for Falcon plasticware (Becton Dickinson, Oxnard, CA).

EM-grade paraformaldehyde was from Electron Microscopy Sciences (Ft. Washington, PA). All other chemicals were analytical grade.

CCK Analogues. The fluorescent ligand probes were synthesized, purified, and characterized as we described previously for the CCK analogue, rhodamine-Gly-[(Nle^{28,31})CCK-26-33] (Rho-CCK) [12], and the CCK receptor antagonist analogue, rhodamine-Gly-[(D-Trp^{30},Nle^{28,31})CCK-26-32]-phenethyl ester (Rho-D-Trp-OPE) [15].

Cell and Tissue Preparations. Chinese hamster ovary cells expressing the rat pancreatic type A CCK receptor (CHO-CCKR cells) have been established and characterized previously [16]. These cells were grown in Ham's F-12 medium in a 37°C humidified incubator containing 5% CO_2. Two days prior to experimental manipulation, cells were plated on glass coverslips and grown to approximately 80% confluence for receptor distribution studies and to approximately 50% confluence for lateral mobility studies.

Pancreatic acinar cells that naturally express CCK receptors were also used in these studies. Dispersed rat pancreatic acini were prepared from male Sprague–Dawley rats (125–150 g) by sequential enzymatic and mechanical dissociation of pancreatic tissue [17]. All procedures involving animals were approved by the Mayo Clinic Animal Care and Use Committee.

Fluorescent Labeling of CCK receptors on CHO-CCKR Cells. CHO-CCKR cells grown on coverslips were washed three times at 37°C with phosphate-buffered saline (PBS) containing 1.5 mM NaH$_2$PO$_4$,8 mM Na$_2$HPO$_4$, 0.145 M NaCl, 0.1 mM MgCl$_2$, and 0.08 mM CaCl$_2$ at pH 7.4. Cells were washed and equilibrated for 10 min with iced PBS in a 4°C cold room prior to incubation with fluorescent ligand for 1 h at 4°C. This provided conditions that allowed surface receptor occupation without internalization. For morphologic studies, the cells were then washed quickly with iced PBS and placed in freshly prepared fixative (2% paraformaldehyde in PBS, pH 7.4) for 30 min at room temperature. Following fixation, coverslips were washed three times with PBS, then mounted on glass slides. Cells were examined using an inverted Zeiss microscope equipped for epifluorescence (Oberkochen, Germany). A 50-W mercury lamp was used for illumination. Specimens were photographed using a 35-mm camera with Tmax 3200 film (Eastman Kodak, Rochester, NY). For control studies, the same labeling procedure was performed on untransfected CHO cells or on receptor-bearing cells in the presence of a 100-fold molar excess of nonfluorescent ligand.

For photobleaching experiments, the CHO-CCKR cells were plated on No. 1 22-mm square glass coverslips

(Baxter, McGaw Park, IL) in individual 35-mm polystyrene dishes (Becton Dickenson, Lincoln Park, NJ). Following fluorescent labeling, coverslips were placed cell side down over a 20 μl (microliter) drop of 4°C PBS on a chilled glass slide. Excess solution was blotted and the coverslip was sealed. Fluorescence recovery studies were performed as described below, immediately following the preparation of these samples.

Fluorescent Labeling of CCK Receptors on Pancreatic Acini. Freshly prepared dispersed rat pancreatic acini were collected by centrifugation at 300 rpm for 3 min, then washed and resuspended in iced enriched Krebs–Ringer–HEPES (KRH) medium containing 25 mM HEPES, pH 7.4, 104 mM NaCl, 5 mM KCl, 1.2 mM MgSO$_4$, 2 mM CaCl$_2$, 1 mM KH$_2$PO$_4$, 0.2% bovine serum albumin, 0.01% soybean trypsin inhibitor, 2.5 mM D-glucose, essential and nonessential amino acids, and 2 mM glutamine. CCK receptors on acinar cells were fluorescently labeled by incubation with 10, 50, or 100 nM Rho-CCK or Rho-D-Trp-OPE at 4°C for 30 min or at 37°C for 15 min in the absence or presence of competing CCK peptides. A drop of the fluorescently labeled cell suspension was place on a chilled glass slide and covered with a No. 0 22-mm square glass coverslip (Baxter). Cells were studied immediately following sample preparation.

Fluorescence Photobleaching Recovery. Fluorescence photobleaching recovery measurements and data analysis were carried out following the procedures described previously [18]. Argon ion laser light of wavelength 514 nm was focused on the cell membrane through a 100× (1.3 NA) oil objective, producing a $1/e^2$ Gaussian beam profile radius of 0.25 μm on the sample. During fluorescence photobleaching recovery experiments, a constant sample temperature was maintained with a temperature-controlled stage. Experiments were usually performed at 10°C except where noted otherwise. To minimize the effect of receptor clustering and redistribution following agonist or antagonist binding, all readings were taken immediately following sample preparation, at a time when fluorescence appeared to be homogeneously distributed over the plasma membrane. Control studies have shown that ligand binding and dissociation kinetics do not appreciably contribute to the observed recovery [11].

Fluorescence photobleaching recovery data were expressed as fractional fluorescence recoveries defined by,

$$f(t) \equiv \frac{F(t) - F(+0)}{F(-) - F(+0)} \qquad (1)$$

where t is time, $F(t)$ is the time-dependent fluorescence intensity, $F(+0)$ is the fluorescence immediately after photobleaching, and $F(-)$ is the prebleach fluorescence. The series solution for $F(t)/F(-)$ and $t \geq 0$, derived for a Gaussian laser beam profile illuminating fluorophores diffusing in two dimensions [19], has

$$F(t)/F(-) = \alpha_0(1 - e^{-K})/K + \sum_{i=1}^{M} \alpha_i \sum_{n=0}^{\infty} [(-K)^n/n!]$$

$$[1 + n(1 + 2t/\tau_{D,i})]^{-1} \qquad (2)$$

where α_0 is the fraction of the total fluorescence (fractional fluorescence yield) contributed by immobilized fluorophores, α_i is the fractional fluorescence yield of the ith mobile component laterally diffusing with relaxation time $\tau_{D,i}$, K is the bleaching depth given by the relation $F(+0)/F(-) = (1 - e^{-K})/K$, and M is the number of mobile components. Equation (2) is appropriate for a system of mobile and immobile fluorophores where all components have identical photobleaching rates. We assume that all fluorophores have identical quantum efficiencies, such that we can equate fractional fluorescence yield with the fractional concentration of labeled molecules. Then the mobile fraction of fluorophores is given by

$$R = 1 - \alpha_0 = \sum_{i=1}^{M} \alpha_i \qquad (3)$$

Finally, the relaxation time and diffusion constant are related by

$$D_i = \frac{\omega^2}{4\tau_{D,i}} \qquad (4)$$

where ω is the Gaussian beam profile radius (= 0.25 μm) on the sample. All data were fitted using Eqs. (1) and (2) using the two-mobile components model ($M = 2$) giving the unknown mobile fractions (α's) and diffusion relaxation times (τ_D's). When one of the mobile fractions was found to be ≤0.05, then the single-mobile component model ($M = 1$) was chosen and the data were reanalyzed. We converted relaxation times to diffusion constants using Eq. (4).

The best-fitting parameters (α's and τ_D's) and their errors were estimated using least-squares minimization [20]. Multiple fluorescence photobleaching recovery curves for a given condition were fitted simultaneously while arriving at the best-fitting solution.

Statistical Analysis. The number of replicate experiments is noted for each figure or presentation of data. Values are expressed as means ± SE of experimental replicates. Significant differences were determined by the Mann–Whitney nonparametric test of unpaired values, with $P < 0.05$ considered to be significant.
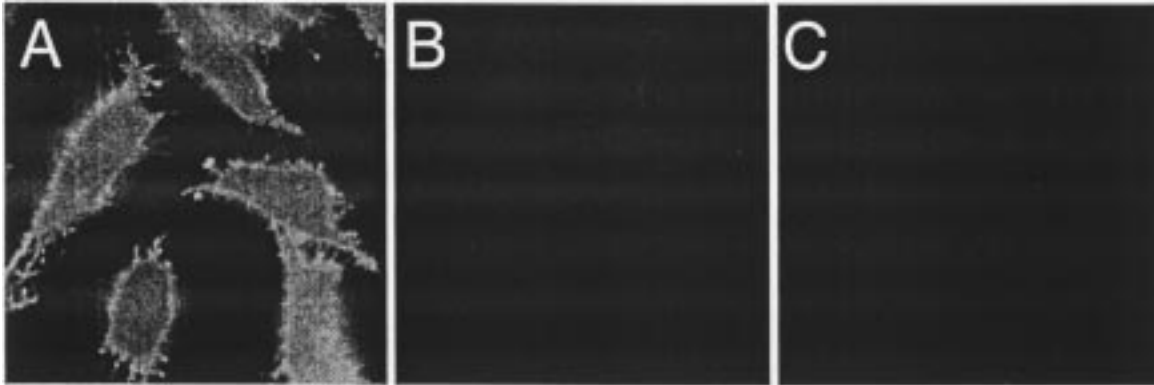
Fig. 1. Fluorescent labeling of CCK receptors on CHO-CCKR cells with Rho-D-Trp-OPE. Shown are fluorescent images of cells labeled for 1 h at 4°C with (A) 2 nM Rho-D-Trp-OPE and (B) 2 nM Rho-D-Trp-OPE plus 200 nM unlabeled D-Trp-OPE. (C) Non-receptor-bearing CHO cells were also incubated for 1 h at 4°C with 2 nM Rho-D-Trp-OPE. Data are representative of three separate experiments.

RESULTS

Morphologic Analysis of CCK Receptor Occupancy with Fluorescent Antagonist. CHO-CCKR cells incubated with 2 nM Rho-D-Trp-OPE at 4°C displayed fluorescent labeling diffusely distributed over the surface of the plasma membrane, including the prominent labeling of membrane protrusions resembling filopodia (Fig. 1A). This labeling was markedly diminished in cells incubated with Rho-D-Trp-OPE in the presence of a 100-fold molar excess of nonfluorescent D-Trp-OPE (Fig. 1B), and no fluorescent labeling of the plasmalemma was observed when this reagent was incubated under identical conditions with non-receptor-bearing CHO cells (Fig. 1C). Similar specificity of labeling of CCK receptors on these cells with the agonist, Rho-CCK, has been demonstrated previously [12]. Morphologic studies

of native pancreatic acini incubated at 4°C with 50 nM Rho-D-Trp-OPE revealed specific basal and lateral plasma membrane fluorescent labeling (Fig. 2) that is analogous to that previously described for acini incubated with Rho-CCK under similar conditions [11]. This labeling was appropriately saturable with excess unlabeled CCK peptides.

Comparison of the labeling intensity of Rho-D-Trp-OPE on CHO-CCKR cells to that of Rho-CCK revealed that antagonist-treated cells were significantly brighter than agonist-treated cells. In terms of fluorescence intensity, cells labeled with 100 nM Rho-D-Trp-OPE at 4°C were approximately 2.8 times brighter than cells labeled with 100 nM Rho-CCK at 4°C (Table I). Intensity levels on native rat pancreatic acinar cells were lower than those observed on CHO-CCKR cells, signifying fewer receptors expressed on the cell surface, as described
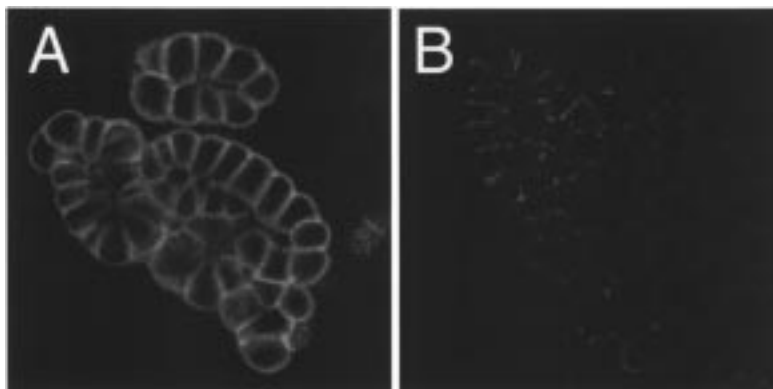

Fig. 2. Fluorescent labeling of CCK receptors on rat pancreatic acinar cells with Rho-D-Trp-OPE. Shown are fluorescent images of acini labeled for 30 min at 4°C with (A) 50 nM Rho-D-Trp-OPE and (B) 50 nM Rho-D-Trp-OPE plus 5 μM unlabeled CCK. Data are representative of three separate experiments.

Table I. Comparison of CCK Receptor Labeling Intensity by Agonists and Antagonists[a]

Ligand	Cell type	Normalized fluorescence intensity	P	n
Rho-CCK	CHO-CCKR	0.35 ± 0.06	—	18
Rho-D-Trp-OPE	CHO-CCKR	1.00 ± 0.12	<0.0001[b]	32
Rho-CCK	Rat pancreatic acini	0.64 ± 0.21	—	7
Rho-D-Trp-OPE	Rat pancreatic acini	1.00 ± 0.43	n.s.[c]	9

[a] Cells were labeled with a 100 nM concentration of the indicated ligand at 4°C prior to fluorescence intensity measurements. Intensity is given as the number of photons counted in a 1-μm-diameter circular area on the plasmalemma in a 250-ms duration. For each cell type, data were normalized by dividing by the average intensity of the Rho-D-Trp-OPE incubation.

[b] Statistical analysis denotes comparison of Rho-CCK and Rho-D-Trp-OPE intensities for CHO-CCKR cells.

[c] Statistical analysis denotes comparison of Rho-CCK and Rho-D-Trp-OPE intensities for pancreatic acini.

previously for Rho-CCK studies on acini [11]. Differences in labeling intensities between agonist and antagonist were less apparent on the native pancreatic acinar cells, although the trend for differences in fluorescence intensity was similar to that observed on the CHO-CCKR cells (Table 1).

Lateral Mobility Characteristics of CCK Receptors on the CHO-CCKR Cell Line. The lateral diffusion of CCK receptors occupied by agonist and antagonist was compared. The recovery curves for CHO-CCKR cells incubated at 4°C with 100 nM Rho-D-Trp-OPE and studied at 10°C were strikingly different from the curves obtained for cells incubated with agonist under similar conditions. A steeper initial slope characterized fluorescence photobleaching recovery curves from Rho-D-Trp-OPE-occupied receptors compared to a more gradual recovery for Rho-CCK-occupied receptors (Fig. 3). Such a rapid increase in fluorescence intensity is characteristic of a rapidly diffusing population of mobile receptors. The agonist and antagonist recovery curves were fitted to estimate the fractional fluorescence yields and diffusion coefficients. These findings are summarized in Table II.

As shown in Table II, diffusion coefficients were significantly different for CCK receptors occupied with these two types of ligands. The parameters determined for CCK receptors labeled with 10 nM Rho-D-Trp-OPE indicated a fast component moving with a lateral diffusion coefficient of $2.6 \pm 0.3 \times 10^{-10}$ cm^2/s and a slow component of $0.1 \pm 0.02 \times 10^{-10}$ cm^2/s. Fast and slow populations of mobile receptors were also noted as the concentration of antagonist was increased to 100 nM. Differences in diffusion coefficients for the slow and fast components at a given concentration were statistically significant for each of the concentrations of Rho-D-Trp-OPE. It is noteworthy that the highest concentration of this fluorescent ligand revealed a rapidly mobile component with a diffusion constant greater than that seen at the lower concentrations. This observation raises the pos-

sibility that a third very rapidly mobile component, made from free ligand associated with the lipid bilayer that had not yet bound to the receptor, might be contributing to these recovery curves.

Careful analysis of the agonist data (previously recognized as only a single mobile state [11]) also demonstrated two distinct populations of mobile receptors for the highest concentration of Rho-CCK (100 nM). At this concentration, a faster component became apparent that might additionally be contributed to by free ligand associated with the lipid in the plasmalemmal bilayer prior to binding to its receptor. Each of the diffusion constants for the agonist ligand was slower than the analogous parameter for the antagonist ligand.

To study further the effects of components of the CCK-stimulated signaling cascade on receptor mobility, we treated CHO-CCKR cells with staurosporine to inhibit phosphorylation by protein kinase C [21]. The observed lateral mobility characteristics of the agonist-occupied CCK receptor under these conditions were most similar to those of the high concentration antagonist-occupied receptor, although substantial variability in the fast component made this parameter not statistically different from that of the agonist-occupied receptor studied in the absence of inhibitor.

Lateral Mobility Characteristics of CCK Receptors on Rat Pancreatic Acini. To examine effects of signaling on receptor diffusion in a natural cellular milieu, we extended our agonist- and antagonist-occupied receptor mobility studies to rat pancreatic acini. Recovery curves for receptors on native pancreatic acini treated at 4°C with 100 nM Rho-D-Trp-OPE did not display the steep initial slope characteristic of a fast component as we had observed on CHO-CCKR cells. Rather, recovery curves observed at 10°C for both agonist- and antagonist-occupied receptors appeared to be distinguished by a single mobile fraction and an immobile fraction.
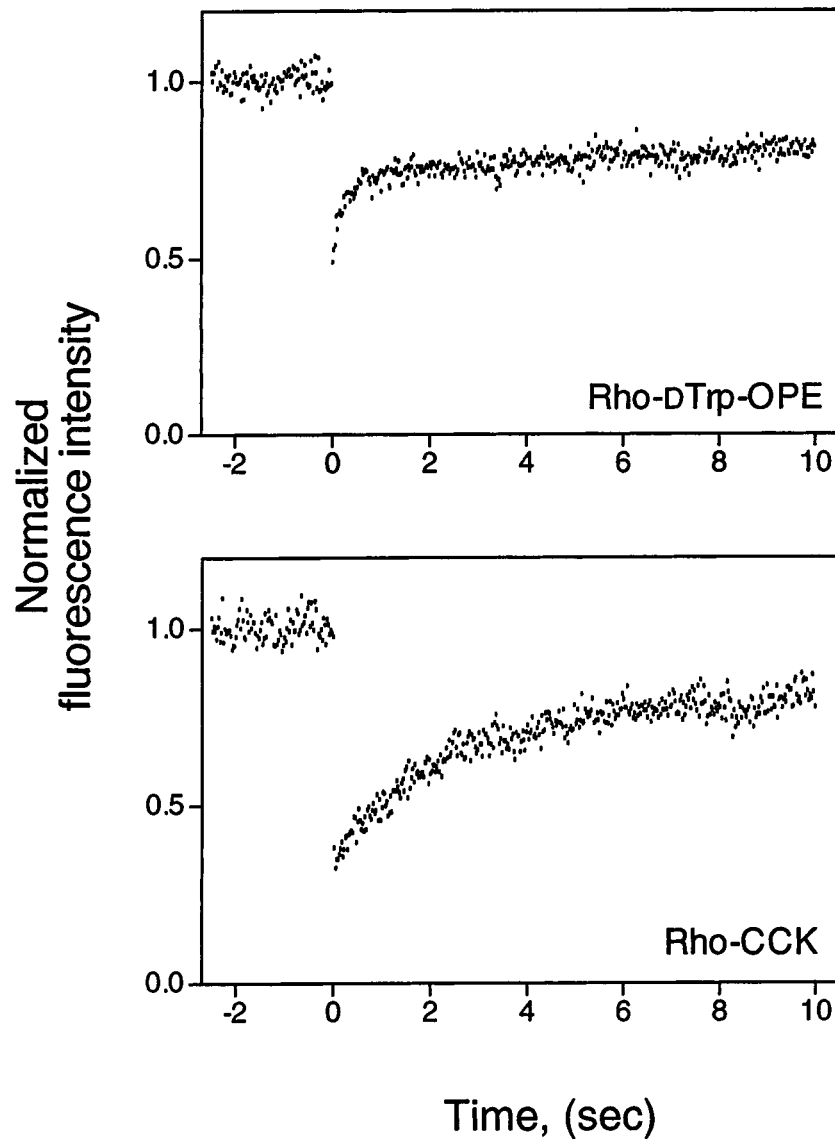
Fig. 3. Typical photobleaching fractional recovery curves showing the diffusion of CCK receptors on CHO-CCKR cells. Cells were grown on coverslips and labeled at 4°C with 100 nM concentrations of fluorescent ligands prior to photobleaching recovery measurements. Filled and open symbols indicate the recovery of receptors labeled with Rho-D-Trp-OPE and Rho-CCK, respectively. Photobleaching recovery measurements were performed on cells at 10°C.

Lateral mobility measurements showed that antagonist-occupied receptors moved in the plane of the plasma membrane at a rate not different from that of the agonist-occupied receptors on native cells (Table III). Acini incubated at 4°C with 50 nM Rho-D-Trp-OPE exhibited single-component mobility characteristics ($D = 0.4 \pm 1.2 \times 10^{-10}$ cm^2/s) that were not different from those determined in previous studies using 50 nM Rho-CCK under analogous conditions ($D = 1.7 \pm 0.4 \times 10^{-10}$ cm^2/s) [11]. The Rho-D-Trp-OPE-occupied mobile receptor

fraction ($R = 0.28 \pm 0.02$) did not differ substantially from the value of R determined previously on acini incubated with 50 nM Rho-CCK under similar conditions ($R = 0.17 \pm 0.05$) [11].

The diffusion coefficients determined for agonist- and antagonist-occupied receptors were also similar at higher ligand concentrations. As shown in Table III, the lateral diffusion coefficient of CCK receptors on acini incubated with 100 nM Rho-D-Trp-OPE ($D = 0.8 \pm 0.5 \times 10^{-10}$ cm^2/s) was not significantly different from

Table II. Diffusion Constants and Mobile Fractions of CCK Receptors on CHO-CCKR Cells[a]

Ligand	Conc. (nM)	D_1 (10^{-10} cm^2/s)	D_2 (10^{-10} cm^2/s)	α_1	α_2	R	n
Rho-D-Trp-OPE	10	2.6 ± 0.3	0.1 ± 0.02	0.61 ± 0.01	0.39 ± 0.01	1.0 ± 0.02	9
Rho-D-Trp-OPE	50	2.4 ± 0.1	0.25 ± 0.02	0.44 ± 0.001	0.56 ± 0.02	1.0 ± 0.03	9
Rho-D-Trp-OPE	100	34 ± 2	1.0 ± 0.2	0.13 ± 0.01	0.60 ± 0.01	0.73 ± 0.02	19
Rho-CCK	10	1.5 ± 0.2	—	0.83 ± 0.01	—	0.83 ± 0.01	7
Rho-CCK	50	1.1 ± 2.1	—	0.90 ± 0.03	—	0.90 ± 0.03	14
Rho-CCK	100	9.4 ± 0.6	0.19 ± 0.02	0.12 ± 0.01	0.88 ± 0.01	1.0 ± 0.02	20
Rho-CCK	50[b]	29.8 ± 11.0	0.6 ± 0.01	0.25 ± 0.02	0.75 ± 0.03	1.0 ± 0.05	7

[a] Diffusion constants (D), fractional concentrations of mobile components (α), and mobile fractions (R) were obtained from the best fits of the fractional fluorescence recovery curves using Eqs. (1)–(4). All data required a two-mobile component fit [$M = 2$ in Eq. (2)] except for the Rho-CCK ligand at 10 and 50 nM, where a single mobile component ($M = 1$) was sufficient. Values represent the mean ± SE for n experiments.
[b] Treatment with 10 M staurosporine prior to and during incubation with Rho-CCK at 4°C.

Table III. Diffusion Constant and Mobile Fraction of CCK Receptors on Pancreatic Acini[a]

Ligand	Conc. (nM)	Temp (°C)	D (10^{-10} cm^2/s)	R	n
Rho-D-Trp-OPE	50	10 ± 2	0.4 ± 1.2	0.28 ± 0.02	8
Rho-D-Trp-OPE	100	10 ± 2	0.8 ± 0.5	0.55 ± 0.01	6
Rho-CCK	100	10 ± 2	1.4 ± 0.1	0.76 ± 0.01	22
Rho-CCK	100	22 ± 2	1.4 ± 0.01	0.85 ± 0.05	7

[a] Notation identical to that in Table II. All data were adequately fitted with the single-mobile component [$M = 1$ in Eq. (2)] model.

the value of D obtained for acini incubated with 100 nM Rho-CCK under similar conditions ($D = 1.4 \pm 0.1 \times 10^{-10}$ cm^2/s). The values of R were 0.55 ± 0.01 and 0.76 ± 0.01 for the antagonist and agonist, respectively.

Of particular interest was the marked increase in the fraction of mobile receptors observed when the concentration of ligand was increased from 50 to 100 nM. This trend was observed in both agonist and antagonist studies. As the fluorescent ligand concentration was increased from 50 to 100 nM, the fraction of Rho-CCK-occupied receptors that were moving in the plane of the plasma membrane increased significantly, from 0.17 ± 0.05 [11] to 0.76 ± 0.01. The same trend was observed in antagonist studies, as the mobile population increased significantly, from 0.28 ± 0.02 to 0.55 ± 0.01. Accordingly, the fraction of mobile receptors became dominant at higher ligand incubation conditions.

DISCUSSION

The lateral mobility of membrane proteins can be affected by their physicochemical characteristics, their interactions with other membrane proteins, their direct or indirect interactions with less mobile molecules residing inside or outside of the cell, obstruction to their movement by noninteracting molecules present in the bilayer (confinement), and fluidity of the lipid bilayer itself [22–25]. Receptors represent a unique group of membrane proteins, since their occupation by a ligand can lead to modification of many of these variables. While both agonists and antagonists may bind to the same receptor molecule, their effects on these variables can be quite distinct. Any type of ligand binding to the receptor may cause conformational changes in the receptor that expose previously hidden domains, and agonist binding may additionally stimulate signaling events that can feedback to modify the receptor molecule and other membrane proteins and that can modify the lipid components of the membrane milieu in which the receptor resides.

There are few examples of the systematic analysis of the lateral mobility of a single receptor molecule occupied by both agonist and antagonist in the same cellular system [26]. In the current report, by performing the comprehensive analysis of the lateral mobility of both antagonist- and agonist-occupied CCK receptors in two types of cells, we have collected novel and potentially quite important data. In addition to receptor that appeared to be immobile within the limitations of the technique of fluorescence recovery after photobleaching, there were at least three diverse states of mobility for the CCK receptor in a single cell under various conditions and

when occupied with distinct types of ligands. These states of receptor mobility varied from cell to cell. The most rapidly moving state was most apparent when the CHO-CCKR cell receptor was occupied by fluorescent antagonist and was more rapid than the predominant state of this receptor when occupied by agonist. This rapidly mobile population of receptors was the major factor contributing to the visually obvious difference in the shape of fluorescence recovery curves generated after photobleaching of the CHO-CCKR cell CCK receptors that had been occupied with antagonist and agonist. There was also a slower laterally mobile state of this receptor that was apparent after both antagonist and agonist occupation, which had indistinguishable characteristics of mobility, and may reflect molecular interactions leading to ultimate immobilization and internalization, known to occur after this receptor is occupied with agonist [12] and antagonist [15]. The intermediate rate of mobility was most apparent after agonist occupation and may reflect molecular interactions key for the processes of signal transduction and receptor regulation.

The most rapidly mobile population of receptors observed in the current work moved at a rate in the order of magnitude that we reported previously for the lateral mobility of lipid in the plasma membrane of the CHO-CCKR cells, using fluorescence recovery after photobleaching of 1,1′-dioctadecyl 3,3,3′,3′-tetramethyl indocarbocyanine perchlorate (DiI) ($D = 8 \pm 0.4 \times 10^{-10}$ cm^2/s) [11]. This population of receptors was observed predominantly with receptor occupation by antagonist. Since antagonists do not initiate any signaling events in the target cell, they are the least likely receptor ligands to stimulate molecular interactions with the receptor. Rapidly mobile states of both fluorescent antagonist and agonist were apparent after incubating the cell with high concentrations of ligands, raising the possibility that some of this signal might reflect free ligand association with the lipid portion of the bilayer, prior to binding to the receptor.

We have performed direct measurements after stimulation with this ligand to demonstrate the absence of stimulation of protein kinase C activity or increase in intracellular calcium [15], both of which have been associated with a reduction in mobility of plasma membrane proteins [27–29]. Indeed, the rapid mobility of the antagonist-occupied CCK receptors is consistent with the absence of critical obstructions or any slowing interactions between the major fraction of these receptors occupied by antagonist and other molecules. It also confirms the relative absence of direct or indirect constraints to the lateral mobility of CCK receptors in these cells, except for the generally recognized effects of the membrane skeleton fence on the mobility of membrane proteins.

Antagonist-occupied *N*-formyl peptide receptors have also been reported to move quite rapidly, presumably on the same basis [26].

The more minor fraction of antagonist-occupied CCK receptors that was observed to move at a slower rate also provides key insights. Recently, we recognized that antagonist occupation of CCK receptors on CHO-CCKR cells results in the internalization of a minor population ($37 \pm 4\%$) via clathrin-dependent endocytosis [15]. It is noteworthy that the portion of such receptors that are internalized [15] is consistent with the portion of antagonist-occupied receptors that were observed to move at this slower rate. Agonist occupation also results in CCK receptor internalization in these cells by the same clathrin-dependent endocytic pathway [12]. The mobility of the population of agonist-occupied receptors was indistinguishable from that of the slower-moving antagonist-occupied receptors. Perhaps the molecular associations that ultimately lead to internalization were similar after occupation with either type of ligand. Presumably the slow mobility is an early step leading to internalization.

A step closer to clathrin-dependent endocytosis of receptors is their immobilization on the cell surface. This is well supported by the literature [26,30,31]. Such complete immobilization likely reflects the clustering of receptors in plasmalemmal areas acquiring a clathrin coat and in coated pits just prior to clearance from the cell surface [26,32,33]. Examples of interactions with components of the clathrin-coated pit and its adapter proteins include Neu receptors [30] and asialoglycoprotein receptors [31]. Indeed, in the current work, we have also identified immobile fractions for both agonist- and antagonist-occupied CCK receptors on the CHO-CCKR cells.

Another quite interesting mobile receptor fraction moved at a rate that was intermediate between the fastest and the slowest components. It was observed after agonist occupation and likely reflects molecular interactions involved in signal transduction and/or changes in the lipid environment brought about by signaling. Precedents exist for both of these phenomena. The heterotrimeric G proteins have been described to associate with components of the cytoskeleton [34]. With G protein association with these receptors the most proximal event in their signaling, this could certainly limit their lateral mobility [35]. More distal events in stimulus–activity coupling pathways, such as kinase activity [36] and increases in intracellular calcium [28,29], also are described to influence membrane dynamics. Decreases in lateral mobility of receptors have been observed with protein kinase C-mediated phosphorylation of immune response receptors [27], tyrosine kinase activity of Neu receptors [30], and agrin-induced phosphorylation of nicotinic acetylcholine receptors [36].

Reduced lipid mobility and increased membrane rigidity have been described in megakaryocyte MEG01 plasma membranes after stimuli that increase intracellular calcium [28,29].

While the themes developed for each of the populations of mobile and apparently immobile CCK receptors on the CHO-CCKR cell seem logical and consistent with our current understanding of signaling and endocytosis; in this work, CCK receptors on pancreatic acinar cells could be classified only as being apparently immobile or being within a single population of mobile receptors. The degree of homogeneity of this group of mobile receptors is not clear. This apparent difference in receptor mobility within the plasma membrane of these two types of cells could be explained in two ways. The differences could be real, based on differences in the composition, organization, or display of key interacting molecules in the cells, or they could reflect limitations in the application of this technique to a cell type with sparse receptors. The density of CCK receptors is known to be approximately 25-fold higher on the CHO-CCKR cell than on the pancreatic acinar cell [16]. Thus, there could be a stoichiometric excess of receptors to regulatory molecules in the cell line, leading to differences in receptor mobility. Actual differences in lateral mobility in the pancreatic acinar cell and the CHO-CCKR cell would also complement the clear differences in receptor handling by these cells. The pancreatic acinar cell retains most of the ligand-occupied receptors on its surface in a specialized microdomain of insulation [11], rather than directing receptors into the endocytic pathway [12]. Other natural cellular locations for the CCK receptor, such as neuronal cells, seem to internalize this receptor quite actively, in a manner analogous to the CHO-CCKR cell [37]. It will be of great interest to direct future studies to extend these types of observations to such cells.

Part of the explanation for the cellular differences in receptor mobility could be methodologic, since the relatively small number of receptors on the acinar cell makes the quantitation less precise, and real differences in rates of mobility of distinct populations of receptors could be hidden. However, while some similar trends observed as significant in the CHO-CCKR cells may be present in the acinar cells, at this time we cannot support such a claim. The major effect on CCK receptor mobility that was observed in this work was the influence of ligand concentration. Incubations with increasing amounts of fluorescent ligand resulted in increasing percentages of mobile receptor. This suggests that the machinery to immobilize the receptor can be limiting, although the molecular interactions that result in the other mobile states are present in stoichiometric excess. As we begin to understand the distinct proteins involved in these processes, this can be better tested.

Additional insights also come from comparisons of different groups of observations in these studies. Receptor–G protein interactions would be expected to occur only with agonists, and not antagonists. The type of mobility observed exclusively with agonist occupation is the intermediate rate of movement. It is possible that this molecular association provides an intermediate constraint on receptor motion, with contributions by secondary interactions between the G protein and the cytoskeleton [34]. Of note, since the antagonist-occupied receptor stimulates internalization, independent of G protein association, the slowest mobility observed with both agonist- and antagonist-occupied receptors is likely independent of G proteins. Similarly, antagonist occupation does not stimulate receptor phosphorylation, while agonist stimulation results in up to 5 mol of phosphate incorporated per mol of CCK receptor [38]. Therefore, molecular interactions with the sites of receptor phosphorylation cannot explain the slowest mobility observed either. These sites are good candidates for intermediate slowing, although treatment with staurosporine, known to reduce CCK receptor phosphorylation by approximately 50% [38,39], had no dramatic effect on this mobility.

These comprehensive observations of mobility of the CCK receptor after occupation with agonist or antagonist in two types of cells provide a better understanding of the types of factors that may contribute to the constraint of receptor motion. Such effects can be important in signaling as well as in the desensitization of the signaling pathway. The cell- and ligand-specific nature of these processes provides additional levels of control to tune both responses and protection mechanisms for the cell. Care should be utilized when interpreting results from photobleaching recovery experiments with different types and concentrations of ligands and when extrapolating results from one type of cell to another.

ACKNOWLEDGMENTS

REFERENCES

1. R. A. Hall, L. S. Ostedgaard, R. T. Premont, J. T. Blitzer, N. Rahman, M. J. Welsh, and R. J. Lefkowitz (1998) *Proc. Natl. Acad. Sci. USA* **95**, 8496–8501.

2. J. A. Pitcher, R. A. Hall, Y. Daaka, J. Zhang, S. S. G. Ferguson, S. Hester, S. Miller, M. G. Caron, R. J. Lefkowitz, and L. S. Barak (1998) *J. Biol. Chem.* **273**, 12316–12324.

3. G. J. Della Rocca, S. Maudsley, Y. Daaka, R. J. Lefkowitz, and L. M. Luttrell (1999) *J. Biol. Chem.* **274**, 13978–13984.

4. R. A. Hall, R. T. Premont, and R. J. Lefkowitz (1999) *J. Cell Biol.* **145**, 927–932.

5. L. M. Luttrell, S. S. Ferguson, Y. Daaka, W. E. Miller, S. Maudsley, R. Della, F. Lin, H. Kawakatsu, K. Owada, D. K. Luttrell, M. G. Caron, and R. J. Lefkowitz (1999) *Science* **283**, 655–661.

6. Y. Tang, L. A. Hu, W. E. Miller, N. Ringstad, R. A. Hall, J. A. Pitcher, P. DeCamilli, and R. J. Lefkowitz (1999) *Proc. Natl. Acad. Sci. USA* **96**, 12559–12564.

7. A. Claing, S. J. Perry, M. Achiriloaie, J. K. Walker, J. P. Albanesi, R. J. Lefkowitz, and R. T. Premont (2000) *Proc. Natl. Acad. Sci. USA* **97**, 1119–1124.

8. I. D. Fraser, M. Cong, J. Kim, E. N. Rollins, Y. Daaka, R. J. Lefkowitz, and J. D. Scott (2000) *Curr. Biol.* **10**, 409–412.

9. S. Maudsley, K. L. Pierce, A. M. Zamah, W. E. Miller, S. Ahn, Y. Daaka, R. J. Lefkowitz, and L. M. Luttrell (2000) *J. Biol. Chem.* **275**, 9572–9580.

10. W. P. Hausdorff, M. G. Caron, and R. J. Lefkowitz (1990) *FASEB J.* **4**, 2881–2889.

11. B. F. Roettger, R. U. Rentsch, E. M. Hadac, E. H. Hellen, T. P. Burghardt, and L. J. Miller (1995) *J. Cell Biol.* **130**, 579–590.

12. B. F. Roettger, R. U. Rentsch, D. Pinon, E. Holicky, E. M. Hadac, J. M. Larkin, and L. J. Miller (1995) *J. Cell Biol.* **128**, 1029–1042.

13. V. Mutt (1980) in G. B. Jerzy Glass (Ed.), *Gastrointestinal Hormones*, Raven Press, New York, pp. 169–221.

14. C. Nagain, M. C. Galas, M. F. Lignon, M. Rodriguez, J. Martinez, and C. Roze (1991) *Pancreas* **6**, 275–281.

15. B. F. Roettger, D. Ghanekar, R. V. Rao, C. Toledo, J. Yingling, D. Pinon, and L. J. Miller (1997) *Mol. Pharmacol.* **51**, 357–362.

16. E. M. Hadac, D. V. Ghanekar, E. L. Holicky, D. I. Pinon, R. W. Dougherty, and L. J. Miller (1996) *Pancreas* **13**, 130–139.

17. M. P. Lutz, S. L. Sutor, R. T. Abraham, and L. J. Miller (1993) *J. Biol. Chem.* **268**, 11119–11124.

18. B. F. Roettger, D. I. Pinon, T. P. Burghardt, and L. J. Miller (1999) *Am. J. Physiol.* **276**, C539–C547.

19. D. Axelrod, D. E. Koppel, J. Schlessinger, E. L. Elson, and W. W. Webb (1976) *Biophys. J.* **16**, 1055–1069.

20. P. R. Bevington (1969) *Data Reduction and Error Analysis for the Physical Sciences*, McGraw–Hill, New York, pp. 204–246.

21. L. K. Gates, C. D. Ulrich, and L. J. Miller (1993) *Am. J. Physiol.* **264**, G840–G847.

22. D. Axelrod (1983) *J. Membr. Biol.* **75**, 1–10.

23. K. Jacobson, A. Ishihara, and R. Inman (1987) *Annu. Rev. Physiol.* **49**, 163–175.

24. J. Van Rampelbergh, P. Poloczek, I. Françoys, C. Delporte, J. Winand, P. Robberecht, and M. Waelbroeck (1997) *Biochim. Biophys. Acta* **1357**, 249–255.

25. R. R. Neubig (1994) *FASEB J.* **8**, 939–946.

26. B. Johansson, M. P. Wymann, K. Holmgren-Peterson, and K. E. Magnusson (1993) *J. Cell Biol.* **121**, 1281–1289.

27. F. Zhang, B. Yang, J. A. Odin, Z. H. Shen, C. T. Lin, J. C. Unkeless, and K. Jacobson (1995) *FEBS Lett.* **376**, 77–80.

28. A. Schootemeijer, A. E. VanBeekhuizen, L. G. Tertoolen, S. W. DeLaat, and J. W. Akkerman (1994) *Eur. J. Biochem.* **224**, 423–430.

29. A. Schootemeijer, A. E. VanBeekhuizen, G. Gorter, L. G. Tertoolen, S. W. DeLaat, and J. W. Akkerman (1994) *Eur. J. Biochem.* **221**, 353–362.

30. L. Gilboa, R. Ben-Levy, Y. Yarden, and Y. I. Henis (1995) *J. Biol. Chem.* **270**, 7061–7067.

31. Z. Katzir, N. Nardi, I. Geffen, C. Fuhrer, and Y. I. Henis (1994) *J. Biol. Chem.* **269**, 21568–21575.

32. A. R. Rees, M. Gregoriou, P. Johnson, and P. B. Garland (1984) *EMBO J.* **3**, 1843–1847.

33. G. Venkatakrishnan, C. A. McKinnon, A. H. Ross, and D. E. Wolf (1990) *Cell Regul.* **1**, 605–614.

34. S. Roychowdhury and M. M. Rasenick (1994) *Biochemistry* **33**, 9800–9805.

35. K.-N. Klotz and A. J. Jesaitis (1994) *BioEssays* **16**, 193–198.

36. T. Meier, G. M. Perez, and B. G. Wallace (1997) *J. Cell Biol.* **131**, 441–451.

37. R. V. Rao, B. F. Roettger, E. M. Hadac, and L. J. Miller (1997) *Mol. Pharmacol.* **51**, 185–192.

38. F. Ozcelebi and L. J. Miller (1995) *J. Biol. Chem.* **270**, 3435–3441.

39. F. Ozcelebi, R. V. Rao, E. Holicky, B. J. Madden, D. J. McCormick, and L. J. Miller (1996) *J. Biol. Chem.* **271**, 3750–3755.